Available online at www.sciencedirect.com

SciVerse ScienceDirect

Procedia Engineering 00 (2012) 000–000

Procedia Engineering

www.elsevier.com/locate/procedia

5th BSME International Conference on Thermal Engineering

Heterogeneous Structure in Diesel Fuel Sprays

Hironobu Ueki[a]*

[a]*Nagasaki University, 1-14 Bunkyo-machi, Nagasaki 852-8521, Japan*

Abstract

A laser 2-focus velocimeter (L2F) has been applied for measurements of velocity and size of droplets in diesel sprays. The maximum data acquisition rate of 15 MHz has been achieved by using FPGA in order to capture every droplet which appears in the micro-scale measurement volume. A method of evaluating the mass flow rate of droplets was proposed, and the distance between droplets was adopted as an indicator of the number density of droplets and the heterogeneous structure of sprays. The diesel fuel spray was injected intermittently into the atmosphere by using a 5-hole injector nozzle. The orifice diameter of the injector nozzle was 0.113 mm, and the injection pressure was set at 40MPa by using a common rail system. Measurements were conducted in the spray on 10 planes from 5 to 25 mm downstream from the nozzle exit. It was shown that the velocity of droplet was the highest at the spray center and decreased towards the spray periphery. The size of droplet at the spray center decreased downstream and that at spray periphery increased downstream. The mass flow rate near the spray center was larger than that in the spray periphery region. It was confirmed that the fuel mass per injection evaluated by the proposed method based on the L2F measurement was nearly equal to the injected mass in a plane further than 15 mm from the nozzle exit. The probability density of droplet with a distance shorter than 5 μm to the adjacent droplet increased remarkably near the spray center 5 and 12 mm downstream from the nozzle exit. It is thought that a region of high number density of droplet exists at the spray center near the spray tip when the spray penetration is shorter than 15 mm.

Keywords: Heat Engine, Droplet, Atomization, Laser Measurement

Nomenclature

d	Diameter of nozzle orifice (mm)
F	Focus diameter (μm)
L	Focus length (μm)
S	Distance between two foci (μm)
T	Time after injection start (ms)
t_1	Time-of-flight (ms)
t_2	Time-of-scattering on the upstream focus (ms)
t_3	Time-of-scattering on the downstream focus (ms)
t	Time (ms)
u	Velocity (m/s)
d_p	Diameter of droplet (μm)
L_d	Distance between droplets (μm)
A	Area (mm^2)
m_f	Mass flow rate

* Corresponding author. Tel.: +81-95-819-2520; fax: +81-95-819-2534.
E-mail address: ueki@nagasaki-u.ac.jp

M	Injected mass (mg/cycle)
N_v	Number of valid data
N_a	Number of all data
x	Coordinate (mm)
y	Coordinate (mm)
z	Coordinate (mm)

1. Introduction

Not only the reduction of exhaust emissions but also further improvement of thermal efficiency is required to diesel engines. As appropriate control of combustion is necessary to meet these requirements, it is important to understand the influence of fuel spray characteristics upon the diesel combustion. Many researchers have investigated about the relation between the injection condition and combustion. For example, the effect of injection pressure on soot formation was reported by Crua, et al. [1]. It has been reported that the high speed fuel spray injected by microscopic hole was effective for further improvement of combustion [6]. Research work is also needed for basic understanding of the spray characteristics. Image processing [7], PDPA [8] and ILIDS [2] are effective as measurement methods of velocity and size of spray droplets. Especially, the information of spray behavior near the nozzle orifice is indispensable for designing the nozzle shape, modeling droplet disintegration and setting the initial condition of simulating droplet disintegration [9,10]. The spatial distribution of the mass in the near-nozzle region was measured by the X- ray radiography technique [3]. There are few studies of the inner structure of the spray where the droplet number density is high.

A laser 2-focus velocimeter (L2F) can measure the time-of-flight when a droplet flies between two foci and gives us the velocity. L2F has the high optical signal to noise ratio, so the influence of multiple scattering on the spray measurement is small. Schodl [11] reported about the application of L2F to the internal flow of turbomachinery in 1974. It was reported by Chaves [12] and Shugger [13] that measurement systems similar to the L2F were successfully applied to measure droplets which were located inside the breakup length. The authors showed that the simultaneous measurements of the velocity and size of droplets were possible by adding the measurement of time-of-scattering to L2F [14].

In the present study, a method of evaluating the mass flow rate of droplets was proposed, and the distance between droplets was adopted as an indicator of the number density of droplets and the heterogeneous structure of sprays. The diesel fuel spray was injected intermittently into the atmosphere by using a 5-hole injector nozzle. The velocity and size of droplets in the spray have been measured by the L2F on 10 planes 5 to 25 mm from the nozzle exit. The spatial distributions of velocity, size, and mass flow rate of droplets have been evaluated, and the region of high number density of droplets has been investigated.

2. Experimental Setup

2.1. Advanced Laser 2-Focus Velocimeter; L2F

The light probe of the L2F consists of highly focused two laser beams as shown in Fig.1. The diameter F of the focus is about 3μm, and the distance S between two foci is 17μm, and the length L is about 20μm in the direction of optical axis. It can be mentioned that the L2F used in the present study has a micro-scale probe. The measurements of time-of-flight and time-of-scattering are shown in Fig.2. The upper half of Fig.2 shows the cross-section of the L2F probe. When a droplet flies through both upstream and downstream foci, time-of-flight t_1, time-of-scattering t_2 on the upstream focus and time-of-scattering t_3 on the downstream focus are measured by a digital counter. The velocity of a droplet can be easily calculated by dividing the distance between two foci S with the measured time-of-flight t_1, that is

$$u = \frac{S}{t_1} \tag{1}$$

The relation used for the estimation of droplet size is that the ratio of the time-of-flight and the time-of-scattering corresponds to the ratio of the distance between two foci S and the droplet size d_p plus the focus size F. The time-of-scattering can be estimated by averaging two time-of-scattering. The droplet size d_p can be estimated by

$$d_p = u \cdot \frac{(t_2 + t_3)}{2} - F \tag{2}$$

The L2F selects a droplet which passes through the upstream focus and downstream focus sequentially. The time-of-fight is shortest when a single droplet passes through two foci, and the time-of-flight is longer when two different droplets pass through two foci. So, a velocity given by different droplets is overestimated and can be removed by a statistical analysis. When the number density of droplet is very high, the local droplet distance is sometimes shorter than the distance between

two foci. In such a case, the droplet other than the droplet which passed the upstream focus will pass the downstream focus. Then, the time-of-flight is not measured correctly. When the flight direction of a droplet is fluctuating, the droplet which passes the upstream focus sometimes differs from the droplet which passes the downstream focus. The velocity obtained by such a pair of different droplets should not be correct. Figure 3 shows the flowchart of the measurements of the time-of-flight and time-of-scattering. Counting starts by the detection of an upstream signal and stops by the detection of a downstream signal, and an up-and-down flag is saved with a counted value. When an upstream signal is detected before detecting a downstream signal, an up-and-up flag is saved with counted value. Valid data can be selected by checking the flag. The sampling data number N_a, which corresponds to the number of the droplets passing through the upstream focus, is set before the measurement.

Figure 4 shows the system configuration of the L2F. The light source is a semiconductor laser which has a maximum power of 100mW and a wave length of 835 nm. A non-spherical lens which has a focal length of 8 mm and a numerical

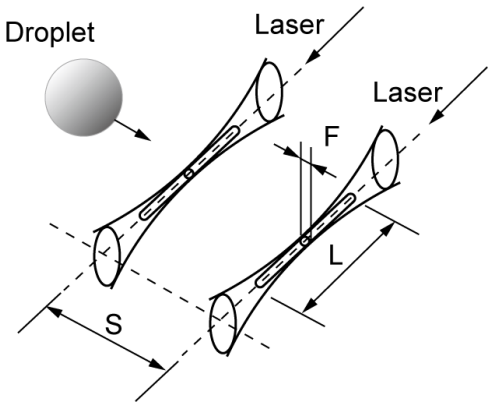

Fig. 1. Light probe of L2F.

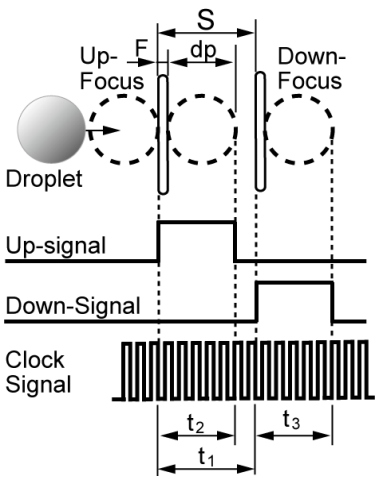

Fig. 2. Time-of-flight and time-of-scattering.

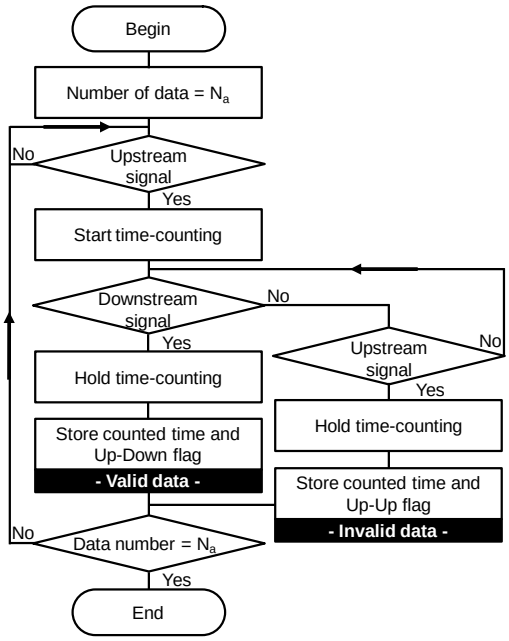

Fig. 3. Flowchart of data acquisition procedure.

aperture of 0.5 is adopted as the condensing lens. By the optical system with a length of 350 mm including the light source, the backscattering light of a droplet at the focus is guided to a Si- APD (Silicon Avalanche Photo Diode), and it is converted into an electrical signal. The time-of-flight and time-of-scattering are measured by the digital counter which is mainly constituted by a FPGA (Field Programmable Gateway Array) with a clock of 160MHz. The maximum data sampling rate of the L2F system is set at 15MHz.

A preliminary experiment has been conducted to confirm the accuracy of size measurement. Droplets generated by a humidifier were seeded in the air flow of about 50 m/s in velocity and they were measured by L2F and PDA (PDI-200MD manufactured by Artium) simultaneously. Figure 5 shows the comparison between probability density distributions of mass-based droplet size measured by L2F and PDA. It is understood that two probability density distributions are very close to each other. The mass-based arithmetic mean sizes measured by L2F and PDA are 9.2 and 9.5 μm respectively. The error in size measurement was 3%. It is understood that the error in mass evaluation is small.

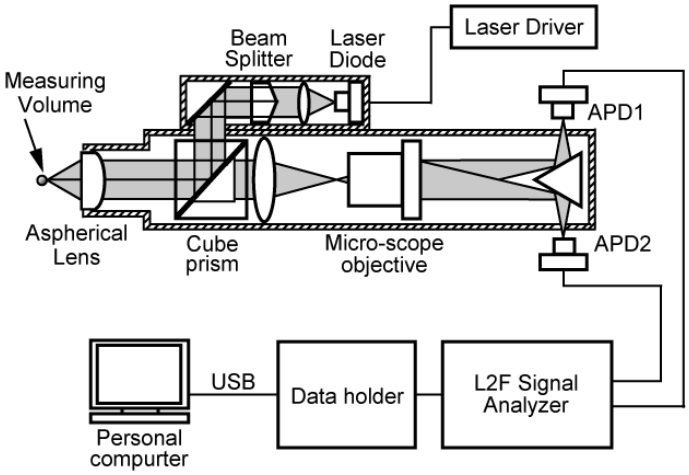

Fig. 4. System diagram of L2F.

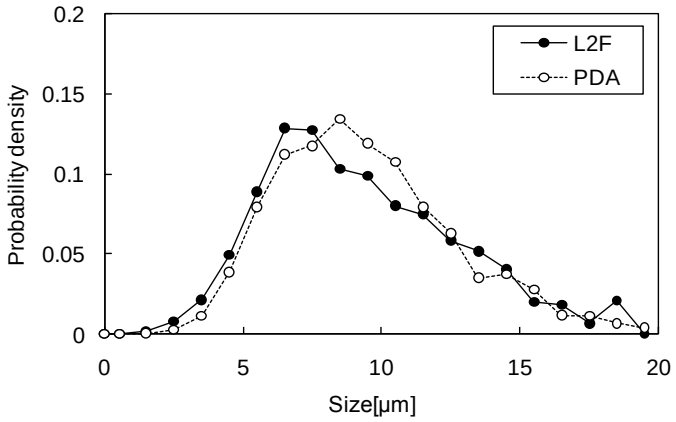

Fig. 5. Probability density distributions of mass-based droplet size measured by L2F and PDA.

2.2. Fuel Spray Measurement System

A common rail injector was used to control injection conditions, such as the injection timing, injection duration and injection pressure. Figure 6 is the measurement system of fuel sprays using the L2F. Diesel fuel pressurized by the high pressure pump was stored in the rail. The rail pressure was set at 40MPa. The fuel was injected intermittently into the atmosphere at a temperature of 298±6K and a pressure of 0.1MPa. The test nozzle was a 5-hole injector with a hole diameter d of 0.113 mm. The measurement of the spray was conducted within one of 5 spray plumes while the remaining 4 plumes were shielded and sucked out through small pipes. The injection interval was 330 ms. The period of energizing the solenoid was 1.0 ms, and the injection period was 0.79 ms. The fuel of 1.34 mg was injected per cycle from one hole. A clock signal with a frequency of 6MHz was used for recording the time when the L2F data was acquired. The number of data N_a was 10,000 at each measurement position. The coordinate z is the distance along the spray axis from the nozzle tip, the coordinate y is the distance along the laser axis, and the coordinate x is perpendicular to y z-axis. The x-axis indicates the radius from the spray center on the plane $y = 0$. Figure 7 shows a spray photograph and measurement positions. There is a dark domain near the position of $z = 5$ mm. This is the shadow of the plug to shield 4 plumes. Simultaneous measurements of velocity and size of spray droplets were conducted on planes perpendicular to z-axis; $z = 5$, 9, 10, 11, 12, 13, 14, 15, 20 and 25 mm. The table 1 shows the x-coordinates of measurement positions in each z plane. The y-coordinates of the measurement positions were fixed to zero. The measurement data were accumulated during 100-1200 injections. In each z plane, $x = 0$ mm corresponds to the spray center, and the most outside measurement position is called the spray periphery.

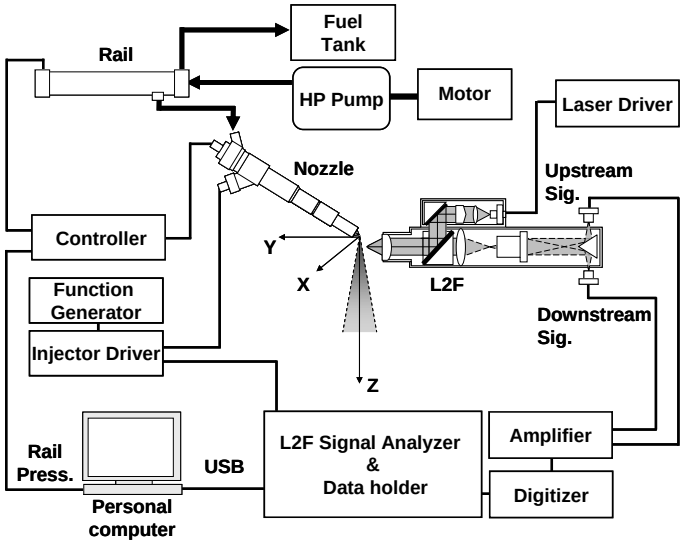

Fig. 6. Fuel spray measurement system.

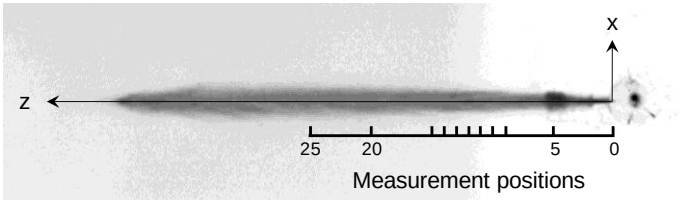

Fig. 7. Spray image and measurement positions (z = 5, 9, 10, 11, 12, 13, 14, 15, 20, 25 mm).

Table 1. Measurement positions.

z(mm)	x(mm)
5	0, ±0.1, ±0.2, ±0.3, ±0.4, ±0.5, ±0.6, ±0.7, ±0.8
9	0, ±0.2, ±0.4, ±0.6, ±0.8, ±1.0
10	0, ±0.2, ±0.4, ±0.6, ±0.8, ±1.0
11	0, ±0.2, ±0.4, ±0.6, ±0.8, ±1.0
12	0, ±0.2, ±0.4, ±0.6, ±0.8, ±1.0
13	0, ±0.2, ±0.4, ±0.6, ±0.8, ±1.0, ±1.2
14	0, ±0.2, ±0.4, ±0.6, ±0.8, ±1.0, ±1.2
15	0, ±0.3, ±0.6, ±0.9, ±1.2
20	0, ±0.4, ±0.8, ±1.2, ±1.6
25	0, ±0.5, ±1.0, ±1.5, ±2.0

2.3. Evaluation of Number Density and Mass Flow Rate

Spatial distribution of droplets is very important for understanding the spray characteristics in a region of high number density droplets and for understanding the processes of evaporation and combustion. A distance L_d between droplets along the direction from upstream focus to downstream focus can be estimated by,

$$L_d = u \cdot \Delta T \tag{3}$$

where ΔT is a time interval between droplet observations and u is an instantaneous velocity.

An important step towards understanding the spray behavior is to estimate the mass flow rate during injection. The mass flow rate is the total mass of droplets passing the measurement probe in a certain time. The mass flow rate m_f estimated as

$$m_f(x,T) = \frac{\rho \cdot \sum V_p(x,T)}{\sum \left(\Delta t(x,T) \cdot \left(L + d_p(x,T)\right) \cdot \left(F + d_p(x,T)\right)\right)} \tag{4}$$

where d_p is the size of droplet, and V_p is the volume of droplet. The total mass M of a single injection can be estimated by the integral of mass flow rate with time and space. When an axisymmetric spray is assumed,

$$M(x,T) = \sum_x \sum_t m_f(x,T) \Delta A(x) \Delta T \tag{5}$$

where ΔA is the cross section of a ring of width Δx which is the distance between the x-coordinate of the measurement positions. The cross section is calculated by

$$\Delta A(x) = 2\pi x \Delta x \tag{6}$$

As shown in Table 1, Δx depends on z. For example, Δx = 0.1 mm in the plane of z = 5 mm. The spray edge was decided on x = ±0.8 mm based on spray images. This was confirmed by the fact that a droplet was not detected at x = ±0.9 mm.

3. Results and Discussion

3.1. Temporal and Spatial Changes in Velocity and Size of Droplets

Figure 8(a) shows the time variation of the mean droplet velocity at 5 positions on the plane z = 5 mm. The mean velocity at the spray center was about 100 m/s at the time T = 0.8 ms, and this is on the same order of magnitude as measured from the spray image. At the points x = 0 mm and x = ±0.4 mm, the mean velocity increased in a period between 0.8 ms and 1.2 ms, and the change in velocity was relatively small in a period between 1.2 and 1.5 ms. The mean velocity decreased rapidly after 1.5 ms and the period after the start of velocity decrease is called period II in this paper. The period before period II is called period I. The period I and period II correspond to so called spray head and spray tail respectively. At the points x = ±0.8 mm, the velocity decreased gradually in a period between 1.0 ms and 1.5 ms. The mean velocities at two measurement positions with the same distance from the spray center, for example x = -1.5 mm and x = 1.5 mm, were nearly the same. Figure 8(b) shows the time variation of the mean droplet velocity at 5 positions on the plane z = 25 mm. The mean velocity at the spray center was about 140 m/s at 1.0 ms. This velocity agreed well with the one which was estimated from the spray images. Droplets appeared at 1.0 ms at the points x = 0, and ±0.5 mm. And they appeared at 1.1 ms at the point x = ±1.5 mm. It is understood that droplets near the spray center reached the measurement position earlier than the droplets in the periphery region. At the positions x = 0 mm and x = ±0.5 mm, the mean velocity increased in a period between 1.0 and 1.2 ms, and the change in velocity was relatively small in a period between 1.2 and 1.5 ms.

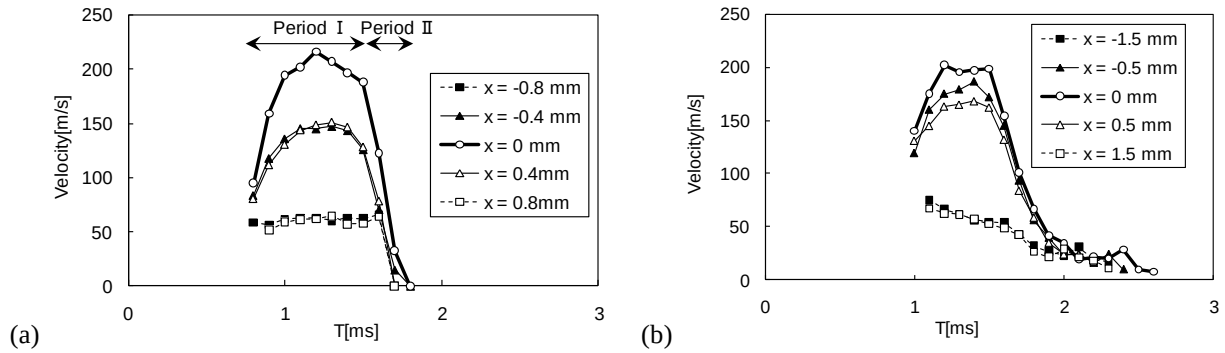

Fig. 8. Time change in Arithmetic mean velocity for (a) z = 5 mm and (b) z = 25 mm.

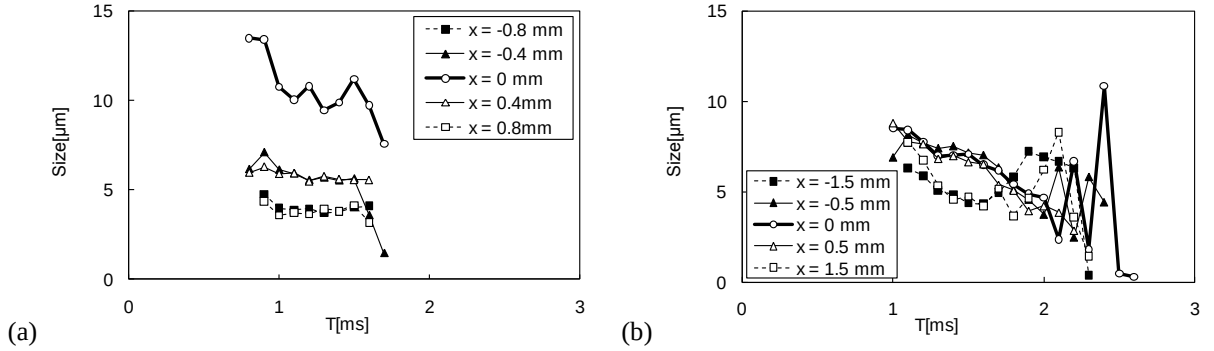

Fig. 9. Time change in Arithmetic mean size for (a) z = 5 mm and (b) z = 25 mm.

Figure 9(a) shows the time variation of the arithmetic mean droplet size on the plane z=5 mm. The mean droplet size when the spray tip reached the measurement position was the largest in the period between 1.0 and 1.5 ms, and the droplet size gradually decreased at every measurement position. Figure 9(b) shows the time variation of the mean droplet size on the plane z=25 mm. The mean droplet size gradually decreased at every measurement position in the first half of the injection duration. The size fluctuated in the latter half of the injection duration.

The time interval between droplets was estimated from the time of droplet observation. Figure 10(a) shows the time variation of the mean time interval within each time window of 0.1 ms on the plane z=5 mm. The time interval at the position x = 0 mm increased in the first half of the injection duration and decreased after that. At positions x = ±0.4 mm, the time interval was shorter than 50 μs during the injection period. At positions x = ±0.8 mm, the time interval decreased in the first half of the injection duration and increased after that. Figure 10(b) shows the time variation of the mean time interval on the plane z=25 mm. At positions x = 0 mm and x = ±0.5 mm, the time interval was between 15 and 50μs in the first half of the injection duration and increased after 1.6 ms. At positions x = ±1.5 mm, the mean time interval decreased in the period between 1.1 ms and 1.3 ms, and increased after 1.3 ms. The time interval between droplets in the spray periphery region was longer than the one at the spray center during the injection period.

The velocity and size in the Period I were used for calculating the mean values at each measurement position, because the temporal change was relatively small. Figure 11(a) shows spatial distributions of the mean velocity on planes z = 5, 10, 15, 20 and 25 mm. The mean velocity showed the highest near the spray center and decreased towards the periphery region. It is understood that the spatial distribution of the mean velocity of droplet is nearly axisymmetry. Figure 11(b) shows the spatial distributions of the arithmetic mean size. On every plane z = constant, it can be seen that the spatial distribution of mean size was nearly axisymmetric as for the one of mean velocity. The mean size showed the largest near the spray center and decreased gradually with the distance from the spray axis towards the periphery region on the plane z = 5 mm. An

increase in size was observed near the spray periphery on planes further than 5 mm from the nozzle exit. Yeh et. al. [4] reported a similar droplet size distribution. It is also understood that the mean size decreased along the spray axis from z = 5 to z = 15 mm.

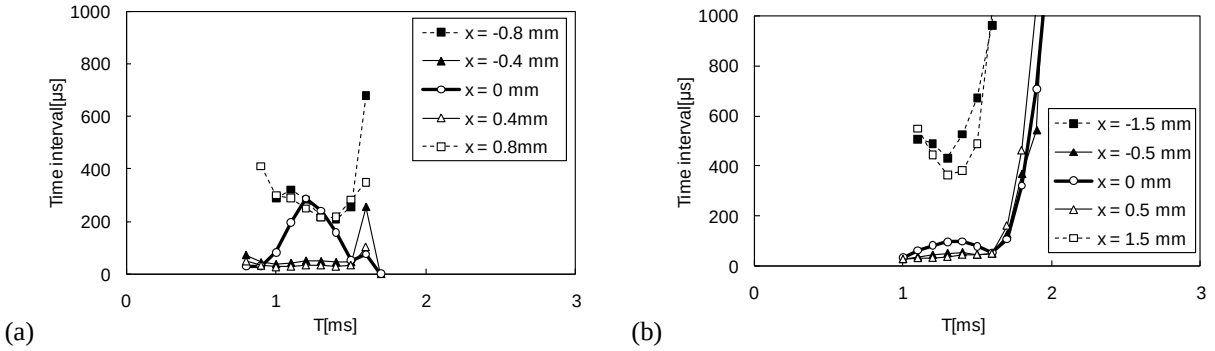

Fig. 10. Time change in Arithmetic mean time interval for (a) z = 5 mm and (b) z = 25 mm.

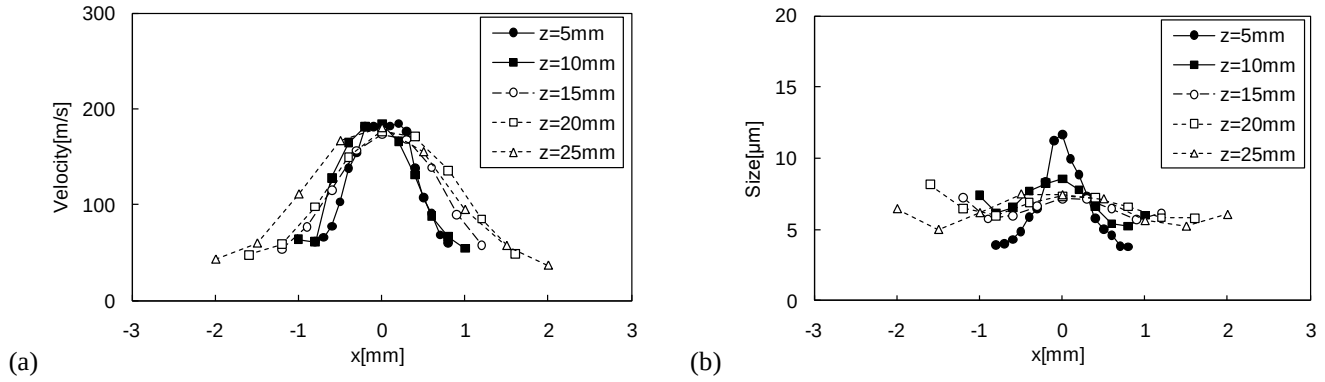

Fig. 11. Spatial distribution in the period I for (a) velocity and (b) size.

3.2. Estimation of Mass Flow Rate

Values of V, d_p and ΔT in the Eqn. (4) for estimating the mass flow rate are given by droplets which passed both upstream and downstream foci. In order to evaluate the mass flow rate of all droplets which passes the measurement volume, it is needed to additionally evaluate the mass of droplets which passed only the upstream focus. Figure 2 shows the ratio of N_v and N_a at each measurement positions on planes z = 5 to 25 mm. The ratio of N_v / N_a was higher than 0.5 near the spray center, although, it decreased to about 0.1 in the spray periphery region. The decrease in the valid data ratio comes mainly from different droplets passing through two foci due to the fluctuation in the direction of droplet flight. The relation between the valid data ratio and the fluctuation of flight direction has been investigated theoretically by Hayami [5]. It was shown that the valid data rate could be estimated to be about 50% when the fluctuation of flight direction was 10 degrees. Therefore, the value of N_v / N_a was thought to be appropriate.

The total mass of droplets passing through the measurement volume is the summation of the mass of droplets passing through both upstream and downstream foci and the mass of droplets passing through only upstream focus. As droplets randomly pass through the measurement volume, it is expected that the mass of droplets is proportional to the number of observed droplets. Accordingly, the mass flow rate of droplets was estimated from the one evaluated by the Eqn. (4) multiplied by N_a / N_v. Figure 13 shows the spatial distribution of the mass flow rate on the plane z = 25 mm within each time window of 0.2 ms. The mass flow rate near the spray center was higher than the one of the spray periphery at each time. The

distribution of mass flow rate can be calculated by integrating time dependent distributions shown in Fig. 13. Figure 14 shows the spatial distribution of mass flow rate on planes z = 5, 10, 15, 20 and 25 mm. It can be seen that the spatial distribution of mass flow rate was nearly axisymmetric. The mass flow rate at the center was the highest at the plane z = 5 mm, and decreased toward the downstream. A peak was not seen on the planes z = 15 - 25 mm, and higher mass flow rates were distributed between positions x = ±0.5 mm.

The fuel mass injected within a single injection can be evaluated by the Eqn. (5). The mass evaluated by the L2F was 1.47mg/injection. As the weighed mass was 1.34mg/injection, the ratio of the evaluated mass and the weighed mass was about 1.1. The error in the evaluation would come from the assumption that the spray is axisymmetric and that the droplet is a sphere. Figure 15 shows the ratio of the evaluated mass and the weighed mass at each measurement position. On measurement planes downstream from the plane z = 15 mm, the ratio of the evaluated mass and the weighed mass was about 1.0. It is understood that almost all droplets were identified by the L2F properly. However, the evaluated mass decreased to less than 1.0 on the planes nearer to the nozzle exit than z = 15 mm. It is understood that unidentified mass increases near the nozzle.

In order to identify the region of high number density of droplets, the distance between surfaces of droplets was estimated by subtracting the droplet size from the distance L_d. Figure 16 shows probability density distribution of the distance between surfaces of droplets at the spray center on planes of z =5, 12, 15, 20 and 25 mm. The probability density of the distance shorter than 20μm on planes z = 5 and 12 mm was higher than that on planes z = 15, 20 and 25 mm. Short distance between droplets means that the number density of droplets is high. It is thought that the laser beam might be scattered by high number density droplets and could not penetrate into the spray center on planes z = 5 and 12 mm. Underestimation of the fuel mass near the nozzle exit should be due to high number density droplets.

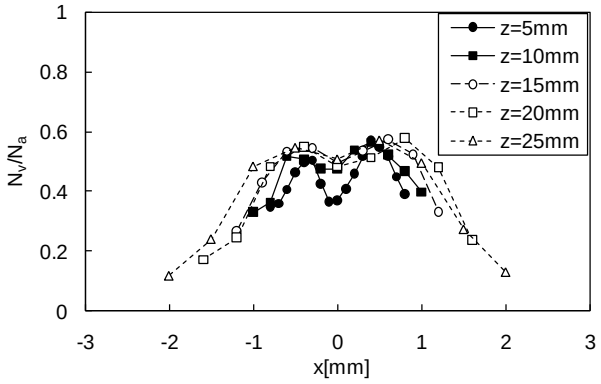

Fig. 12. Ratio of valid data number and all data number; Period I.

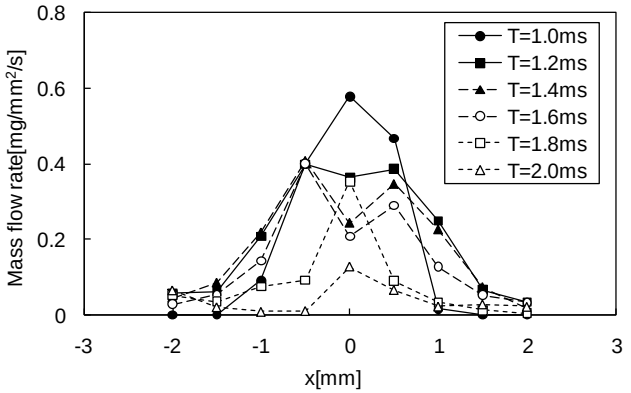

Fig. 13. Spatial distribution of mass flow rate; z = 25 mm.

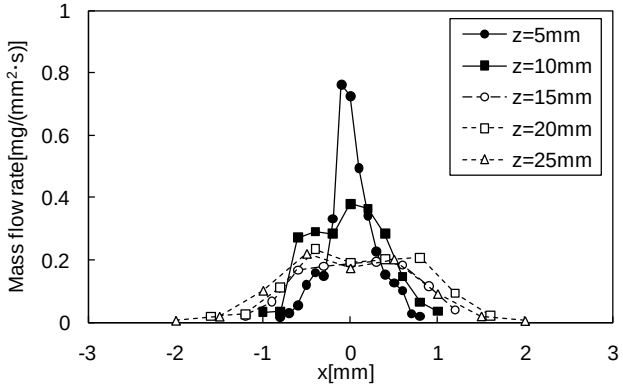

Fig. 14. Spatial distribution of mass flow rate.

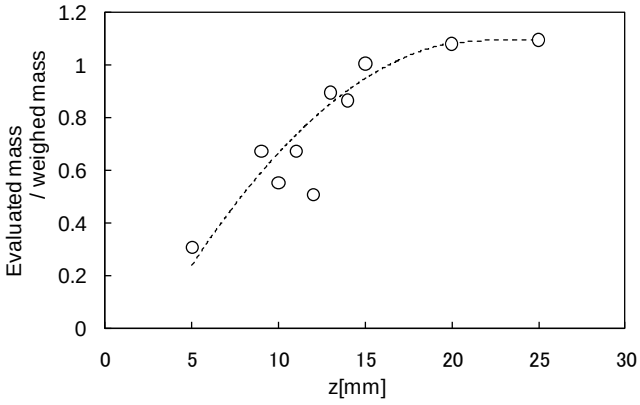

Fig. 15. Ratio of evaluated mass per injected mass.

Figure 17(a) shows the probability density distribution of the distance between surfaces of droplets at 5 positions x = 0.0,0.1, 0.2, 0.3 and 0.4 mm on the plane z = 5 mm. It is clearly seen that the probability density of the distance shorter than 20μm at the position x = 0.0 mm was higher than that at positions x = 0.1, 0.2, and 0.4 mm. It is thought that a region of high number density of droplets exists inside of the position x = 0.1 mm. That is, the diameter of the high number density region can be thought as an order of 0.1 mm on z = 5 mm. Figure 17(b) shows the probability density distribution of the distance between surfaces of droplets at 4 positions x = 0.0, 0.2, 0.4 and 0.6 mm on the plane z = 12 mm. The probability densities of the distance shorter than 10μm at positions x = 0.0 and 0.2 mm were relatively higher than that at positions x = 0.4 and 0.6 mm. Figure 18 shows the time variation of the probability density of droplets with a distance between their surfaces shorter than 5μm at the spray center on planes z = 5 and 12 mm. It is understood that the region of high number density of droplet appeared at the time when the spray tip reached the measurement position. In other words, a region of high number density of droplets is thought to exist at the spray center near the spray tip when the spray penetration is shorter than 15 mm.

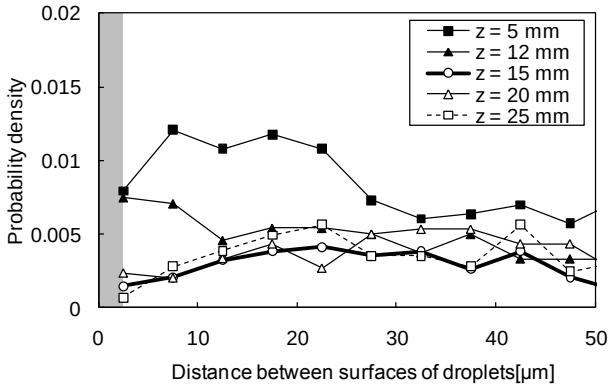

Fig. 16. Probability density of distance between surfaces of adjacent droplets ; x=0 mm.

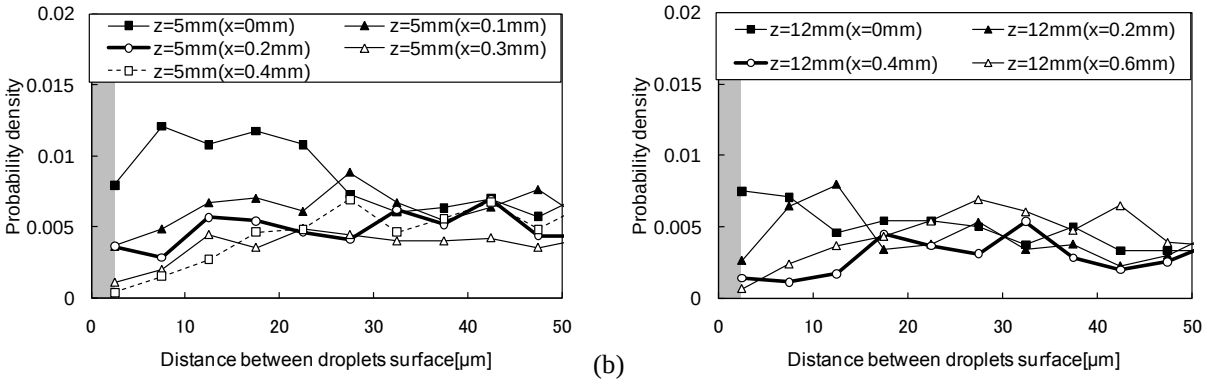

Fig. 17. Probability density of distance between surfaces of adjacent droplets for (a) z = 5 mm and (b) z = 25 mm.

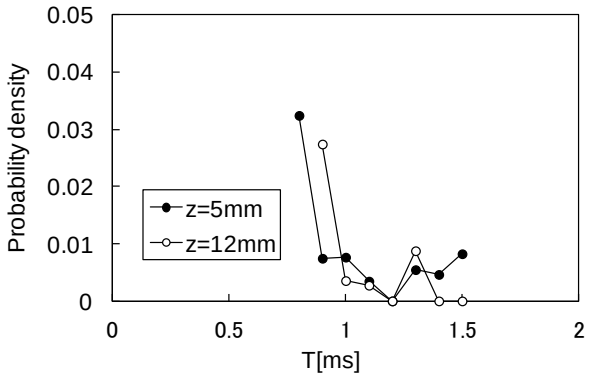

Fig. 18. Probability density of droplets with a distance between their surfaces shorter than 5μm at the spray center.

4. Conclusions

A L2F has been utilized for measurements of velocity and size of droplets in diesel fuel sprays injected under a common rail pressure of 40MPa. A method of evaluating the mass flow rate of droplets was proposed, and the distance between droplets was adopted as an indicator of the number density of droplets and the heterogeneous structure of sprays. Measurements were conducted inside sprays on 10 planes from 5 to 25mm downstream from the nozzle exit. Based on the measurement of temporal changes in velocity and size of droplets, mean values of velocity and size at each measurement position were evaluated. The results showed that the velocity of droplet was the highest at the spray center and decreased towards the spray periphery. The size of droplet at the spray center decreased downstream and that at spray periphery increased downstream. The mass flow rate near the spray center was larger than that in the spray periphery region. The fuel mass per injection evaluated by the proposed method based on the L2F measurement was nearly equal to the weighed mass on planes further than 15 mm from the nozzle exit. It is thought that a region of high number density of droplet exists at the spray center near the spray tip when the spray penetration is shorter than 15 mm. The effect of injection conditions such as the injection pressure, ambient pressure, and nozzle hole diameter on the heterogeneous structure of sprays will be investigated in a future work.

References

- Journal articles:

[1] Crua, C., Kennaird, D.A., Heikal, M.R., 2003. Laser-induced incandescence study of diesel soot formation in a rapid compression machine at elevated pressures, Combustion and Flame, 135(4), pp.475-488

[2] Ryu, C-S., Moriyoshi, Y., Aoyanagi, Y., 2007. 2D Simultaneous Measurements of Droplets Diameter and Velocity in a Diesel Spray by Using Improved ILIDS Method, Transactions of the Japan Society of Mechanical Engineers, Series B, 73-725, pp.380-386

[3] [10] Kastengren, A. L., Powell, C. F., Im, K.-S., Wang, Y.-J., Wang, J., 2009. "Measurement of Biodiesel Blend and Conventional Diesel Spray Structure Using X-Ray Radiography", Journal of Engineering for Gas Turbines and Power, Vol.131, pp.0628021-0628027.

- Edited Book:

[4] Yeh, C., N., Kosaka, H., Kamimoto, T., 1996. Measurement of Drop Sizes in Unsteady Dense Sprays, in "*Recent Advances in Spray Combustion: Spray Atomization and Drop Burning Phenomena*", Kuo, K., Editor. AIAA, Vol.1, pp.297-308.

[5] Hayami, H., Hirashima. K., 1987. Velocity Measurements in Combustion Fields Using a Laser-2-Focus Velocimeter, in "*Laser Diagnostics and Modeling of Combustion*", Inamura, K., Editor. Springer-Verlag, pp.21-28.

- Symposium Proceedings:

[6] Fezzaa, K., Lee, W-K., Cheong, S-K., Powell, C.F., Lai, M-C., Wang, J., 2005. "High-Pressure Diesel Injection Studied by Time-Resolved X-Ray Phase-Contrast Imaging", Proceedings of ILASS-Asia, pp.209-212.

[7] Choongsik, B., Jun, Y., Jangsik, K., Kyeong, O, L., 2002. "Effect of Nozzle Geometry on the Common-Rail Diesel Spray", SAE Paper , No.2002-01-1625

[8] Takeda, T., Okumura, N., Senda, J., 2006. "Study on Droplet Measurement of Unsteady Diesel Spray Using Phase Doppler Anemometry (PDA)" , Proceedings of ICLASS, ICLASS-06-118, p.233.

[9] Han, J-S., Lu, P-H., Xie, X-B., Lai, M-C. Henein, N.A., 2002. "Investigation of Diesel spray Primary Break-up and Development for Different Nozzle Geometries", SAE Paper No.2002-01-2775

[10] Lacoste, J., Crua, C., Heikal, M., Kennaird, D., Gold, M., 2003. "PDA Characterisation of Dense Diesel Sprays Using a Common-Rail Injection System", SAE Paper , No.2003-01-3085 , pp.2074-2085.

[11] Shodl, R., 1974. "L2FA Laser-Dual-Beam Method for Flow Measurements in Turbomachines", ASME Paper No.74-GT-157.

[12] Chaves, H., Kirmse, C., Obermeier, F., 2001, "Velocity Measurements of Dense Diesel Sprays in Pressurized Air", Proceedings of Spray 2001, TU Hamburg-Harburg, pp. II. 2-1-II. 2-8.

[13] Schugger, C., Meingast, U., Renz, U., 2000. "Time-Resolved Velocity Measurements in the Primary Breakup Zone of a High Pressure Diesel Injection Nozzle", Proceedings of ILASS-Europe, Darmstadt, pp.1-5.
[14] Ueki, H., Ishida, M., Sakaguchi, D., 1994. "Simultaneous Measurement of Particle Size and Velocity by Laser 2-Focus Particle Analyzer", Proceedings of ICLASS 1994, pp.483-490.